Optics Communications 310 (2014) 90–93

Contents lists available at ScienceDirect

Optics Communications

journal homepage: www.elsevier.com/locate/optcom

Manipulation of terahertz pulse generation in ZnTe crystal by shaping femtosecond laser pulses with a square phase modulation

Chenhui Lu [a], Shian Zhang [a,*], Tianqing Jia [a], Jianrong Qiu [b], Zhenrong Sun [a]

[a] *State Key Laboratory of Precision Spectroscopy, and Department of Physics, East China Normal University, Shanghai 200062, People's Republic of China*
[b] *State key Laboratory of Luminescent Materials and Devices, and Institute of Optical Communication Materials, South China University of Technology, Wushan Road 381, Guangzhou 510640, People's Republic of China*

ARTICLE INFO

Article history:
Received 12 June 2013
Received in revised form
22 July 2013
Accepted 27 July 2013
Available online 8 August 2013

Keywords:
Terahertz pulses
Pulse shaping
Coherent control

ABSTRACT

We theoretically demonstrate that the terahertz pulse generation via optical rectification in ZnTe crystal can be effectively controlled by making use of the shaped femtosecond laser pulses with a square phase modulation. We show that, by precisely controlling these parameters characterizing the square phase modulation, the terahertz spectrum is periodically modulated and the terahertz pulses are split into multiple subpulses, and the modulation period of the terahertz spectrum and the relative intensity and time interval of these terahertz subpulses can be continuously tuned. Furthermore, we utilize the power spectrum of the shaped femtosecond laser pulses to explain the physical control mechanism of the shaped and tunable terahertz pulse generation.

Terahertz radiation with the spectral range from 0.1 to 10 THz or 3 to 300 cm^{-1} falls in between infrared radiation and microwave radiation in the electromagnetic spectrum, and therefore it shares some properties of both the two radiations. Because of the lack of high quality terahertz sources and efficient detectors, the study and application of terahertz pulses have been greatly restricted. Recently, with the advent of the femtosecond laser technique, the reliable terahertz pulses can be obtained by photoconductive switches [1,2], optical rectification (OR) [3] or photo-induced plasma in a gaseous medium [4,5]. Now, the terahertz pulses have been widely applied to various fields, such as non-invasive imaging [6,7], communication [8,9], molecular spectroscopy [10,11], high-speed optical signal processing [12,13], biological and medical imaging [14,15], and non-destructive evaluation (NDE) [16].

For some specific applications of the terahertz pulses, such as collective coherent control over ferroelectric domain orientation and material structure [17], it is necessary to generate the arbitrarily shaped and tunable terahertz pulses. Nowadays, two primary techniques have been proposed to generate the shaped or tunable terahertz pulses. One is using pre-engineered orientation-inverted nonlinear optical media with poled lithium niobate to synthesize terahertz waveform [18,19], and the terahertz waveform is consistent with the crystal domain structure. For example, Lee et al. obtained the zero-area double, chirped and alternating terahertz pulses via optical rectification in poled ferroelectric crystal [18]. The other is employing the coherent control strategy based on the femtosecond pulse shaping technique [20–22]. When the shaped femtosecond laser pulses propagate in the nonlinear crystal or photoconductive switch, the shaped and tunable terahertz pulses can be generated by varying the laser spectral phase. For example, Ahn et al. realized the tailored terahertz pulses using the adaptive feedback control method based on a Gerchberg–Saxton algorithm, including chirped pulses, zero-area pulses and trains of multiple pulses [21]. Vidal et al. obtained the terahertz pulse train by a sinusoidal or triangular phase modulation [22].

In this paper, we employ the shaped femtosecond laser pulses with a square phase modulation to generate the shaped and tunable terahertz pulses via optical rectification in the ZnTe crystal. This square phase modulation has been proven to be a well-established tool in quantum control because it can obtain such a shaped femtosecond laser pulse train with the tunability in relative intensity and time interval of these subpulses [23–25]. Our results show that, by the square phase modulation, the terahertz spectrum is periodically modulated and the terahertz pulses are split into multiple subpulses. By varying the modulation depth and modulation period of the square phase modulation, the modulation period of the terahertz spectrum and the relative intensity and time interval of the terahertz subpulses can be continuously tuned. Furthermore, the physical control mechanism of the shaped and tunable terahertz pulse generation is discussed and analyzed by considering the power spectrum of the shaped femtosecond laser pulses.

* Corresponding author. Tel.: +86 21 62233210; fax: +86 21 62232056.
E-mail addresses: sazhang@phy.ecnu.edu.cn (S. Zhang), zrsun@phy.ecnu.edu.cn (Z. Sun).

0030-4018/$ - see front matter © 2013 Elsevier B.V. All rights reserved.
http://dx.doi.org/10.1016/j.optcom.2013.07.075

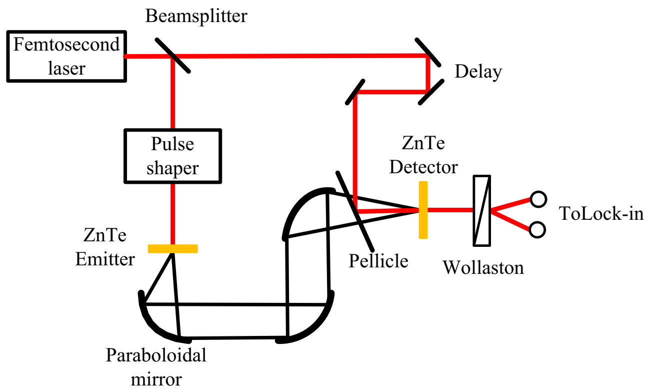

Fig. 1. Experimental setup for the generation of the shaped and tunable terahertz pulses by the femtosecond pulse shaping technique.

Our theoretical simulation is based on the experimental setup of the general terahertz pulse shaping [21,22], as shown in Fig. 1. A Ti:sapphire mode-locked laser is used as the excitation source with the pulse duration of 35 fs and the central frequency of 379.7 THz (corresponding to the laser central wavelength of 790 nm). The output femtosecond laser pulses are spilt two components by a beamsplitter, one component is tailored by a pulse shaper and used to generate the shaped and tunable terahertz pulses via optical rectification in a ⟨110⟩ ZnTe crystal, and the shaped and tunable terahertz pulses in time and frequency domains are measured via electro-optical (EO) effect in a second ZnTe crystal by applying the other unshaped component. Here, the thicknesses of the two ZnTe crystals are both set to be $L_e = L_d = 300$ μm.

Based on Freysz's theoretical model [22,26], the generated terahertz spectrum via optical rectification in the ⟨110⟩ ZnTe crystal can be expressed by

$$E_{THz}(\Omega) = iL_e \frac{\Omega^2}{c^2} \frac{\chi^{(2)}(\Omega)}{k(\Omega)+\Omega/v_g} e^{i[k(\Omega)+\Omega/v_g]L_e/2} C(\Omega) \sin c\left[\frac{L_e \Delta k}{2}\right], \quad (1)$$

where c is the velocity of light in vacuum, v_g is the group velocity of the laser pulses in the ZnTe crystal, $\chi^2(\Omega)$ is the frequency dependence nonlinear susceptibility, and $\Delta k = k(\Omega) - \Omega/v_g$ is the phase mismatch between the terahertz pulses and the laser pulses. In time domain, the terahertz waveform via the EO effect in the second ZnTe crystal can be written as

$$S(\tau) = \int_{-\infty}^{+\infty} S(\Omega) e^{-i\Omega\tau} d\Omega, \quad (2)$$

where τ is the time delay between the terahertz pulses and the probe laser pulses, $S(\Omega)$ is the detected EO signal spectrum [27], and is given by

$$S(\Omega) = E_{THz}(\Omega) C_{probe}(\Omega) \chi^2(\Omega) \frac{e^{iL_d \Delta k} - 1}{i\Delta k}, \quad (3)$$

where $C(\Omega)$ and $C_{probe}(\Omega)$ respectively represent the power spectra of the excitation pulses and the probe pulses, and are written as

$$\begin{aligned} C(\Omega) &= \int_{-\infty}^{+\infty} d\omega E(\omega) E^*(\omega - \Omega)/2\pi \\ &= \int_{-\infty}^{+\infty} d\omega A(\omega) A(\omega - \Omega) e^{i[\Phi(\omega) - \Phi(\omega - \Omega)]}/2\pi \end{aligned} \quad (4)$$

where $A(\omega)$ and $\Phi(\omega)$ are the laser spectral amplitude and phase in frequency domain, respectively. It is easy to verify that $C(\Omega)$ is maximal value for the transform-limited laser pulses (i.e., $\Phi(\omega) = 0$) and other spectral phase distributions will reduce and even eliminate it. Since the terahertz pulse generation (i.e., $S(\tau)$ or $S(\Omega)$) depends on the power spectrum $C(\Omega)$, as shown in Eqs. (3) and (4), it can be effectively controlled by varying the laser spectral phase. Here, we utilize a square phase modulation to control the terahertz pulse generation, as shown in Fig. 2(a). In mathematics, the square phase modulation can be defined by the function of

$$\Phi(\omega) = \frac{\alpha}{2} + \frac{2\alpha}{\pi} \sum_{l=0}^{\infty} \frac{\sin[\beta(2l+1)(\omega - \omega_0)]}{(2l+1)}, \quad (5)$$

where α and β respectively represent the modulation depth and modulation period, and ω_0 is the laser central frequency. In time domain, the square phase modulation can produce the controllable subpulse sequences, as shown in Fig. 2(b). The modulation depth α is controlling the relative intensity between the central subpulse and these side subpulses, and the central subpulse vanishes while these side subpulses reach maximal value when $\alpha = \pi$. The modulation period β is controlling the time interval of these subpulses, and the time interval increases with the increase of β.

We first demonstrate the effect of the modulation depth α on the terahertz pulse generation. Fig. 3 shows the terahertz spectra $|S(\Omega)|^2$ induced by the shaped femtosecond laser pulses with the modulation period $\beta = 1$ THz for different modulation depths: (a) $\alpha = 0$ (purple solid line), 0.2π (green dashed line), 0.3π (blue dotted line) and 0.5π (red dash-dotted line), and (b) $\alpha = 0.6\pi$ (purple solid line), 0.7π (green dashed line), 0.8π (blue dotted line) and π (red dash-dotted line). As can be seen, with the increase of modulation depth from $\alpha = 0$ to 0.5π, as shown in Fig. 3(a), these terahertz spectral intensities at the frequencies of $\Omega/2\pi = 0.5$, 1.5, 2.5 and 3.5 THz are reduced and reach to zero level at $\alpha = 0.5\pi$, while these terahertz spectral intensities at the frequencies of $\Omega/2\pi = 1$, 2 and 3 THz keep unchanged. Thus, a periodically modulated terahertz spectrum is obtained, and the modulation period is 1 THz. However, when the modulation depth is changed from $\alpha = 0.5\pi$ to π, as shown in Fig. 3(b), these terahertz spectral intensities at the frequencies of $\Omega/2\pi = 0.5$, 1.5, 2.5 and 3.5 THz gradually recover and reach to the maximal value that excited by the transform-limited laser pulses at $\alpha = \pi$, and therefore the modulation period of the terahertz spectrum becomes 0.5 THz, which is half of that at $\alpha = 0.5\pi$.

Fig. 4 presents the corresponding terahertz waveforms $|S(\tau)|^2$ induced by the shaped femtosecond laser pulses with the same

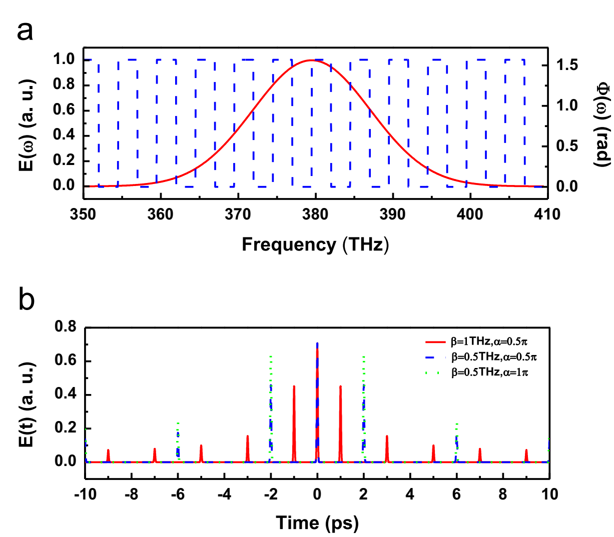

Fig. 2. (a) The square phase modulation applied on the laser spectrum with the modulation depth $\alpha = 0.5\pi$ and the modulation period $\beta = 5$ THz. (b) The temporal intensity profile of the shaped femtosecond laser pulses for $\alpha = 0.5\pi$ and $\beta = 1$ THz (red solid line), $\alpha = 0.5\pi$ and $\beta = 0.5$ THz (blue dashed line), and $\alpha = \pi$ and $\beta = 0.5$ THz (green dotted line). (For interpretation of the references to color in this figure legend, the reader is referred to the web version of this article.)

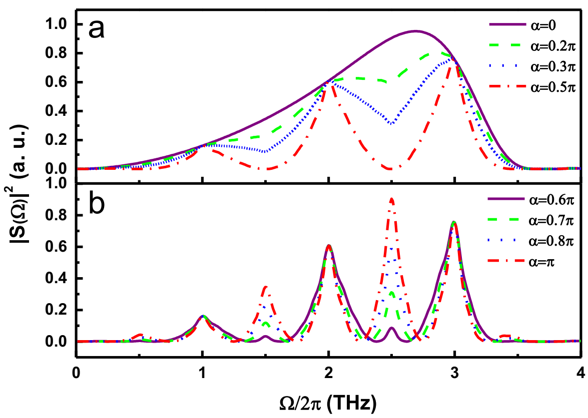

Fig. 3. The terahertz spectra $|S(\Omega)|^2$ induced by the shaped femtosecond laser pulses with the modulation period $\beta=1$ THz for different modulation depths: (a) $\alpha=0$ (purple solid line), 0.2π (green dashed line), 0.3π (blue dotted line) and 0.5π (red dash-dotted line), and (b) $\alpha=0.6\pi$ (purple solid line), 0.7π (green dashed line), 0.8π (blue dotted line) and π (red dash-dotted line). (For interpretation of the references to color in this figure legend, the reader is referred to the web version of this article.)

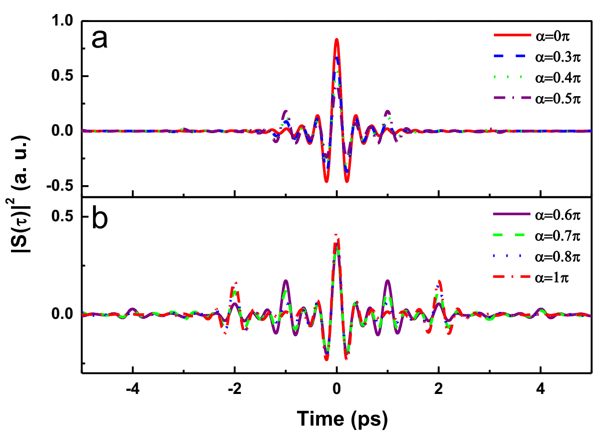

Fig. 4. The corresponding terahertz waveforms $|S(\tau)|^2$ induced by the shaped femtosecond laser pulses with the same modulation parameters in Fig. 3.

modulation parameters in Fig. 3. Because of the periodical modulation of the terahertz spectrum, the terahertz pulses are split into multiple subpulses. When the modulation depth is changed from $\alpha=0$ to 0.5π, as shown in Fig. 4(a), the central subpulse at the time of $\tau=0$ ps is suppressed while the two side subpulses at the time of $\tau=-1$ and 1 ps are enhanced, which are maximally suppressed and enhanced at $\alpha=0.5\pi$, respectively. When the modulation depth is changed from $\alpha=0.5\pi$ to π, as shown in Fig. 4(b), the central subpulse at the time of $\tau=0$ ps almost keeps unchanged, but the two side subpulses at the time of $\tau=-1$ and 1 ps are suppressed and simultaneously two new side subpulses at the time of $\tau=-2$ and 2 ps are generated, and the two side subpulses at the time of $\tau=-1$ and 1 ps vanish and the two new side subpulses at the time of $\tau=-2$ and 2 ps reach maximal value at $\alpha=\pi$. By comparing the terahertz waveforms at $\alpha=0.5\pi$ and π, one can see that the time interval of these subpulses at $\alpha=\pi$ is twice of that at $\alpha=0.5\pi$.

Next we study the dependence of the terahertz pulse generation on the modulation period β. Here, we only consider these representative cases with the modulation depths $\alpha=0.5\pi$ and π. Fig. 5 shows the terahertz spectra $|S(\Omega)|^2$ induced by the shaped femtosecond laser pulses with the modulation depths $\alpha=0.5\pi$ (a-1) and π (a-2) for the modulation periods $\beta=0.5$ THz (red dotted line), 1 (blue dashed line) and 2 (green solid line), and the corresponding terahertz waveforms $|S(\tau)|^2$ (b-1) and (b-2). As can be seen, with the increase of the modulation period β, the modulation period of the terahertz spectrum decreases while the time interval of the terahertz subpulses increases. That is to say, by varying the modulation period β, the modulation period of the terahertz spectrum and the time interval of the terahertz subpulses can be continuously tuned, which is very useful for the future applications of the terahertz pulses. Again, one can see that the modulation period of the terahertz spectrum at $\alpha=0.5\pi$ is twice of that at $\alpha=\pi$ while the time interval of the terahertz subpulses at $\alpha=0.5\pi$ is half of that at $\alpha=\pi$ for a given modulation period β. Moreover, it can be found that the modulation period of the terahertz spectrum T_{mod} and the modulation period of the square phase modulation β exist the relation of $T_{\text{mod}}=\beta$ at $\alpha=0.5\pi$ and $T_{\text{mod}}=0.5\beta$ at $\alpha=\pi$ while the time interval of the terahertz subpulses τ_{mod} and the modulation period β exist the relation of

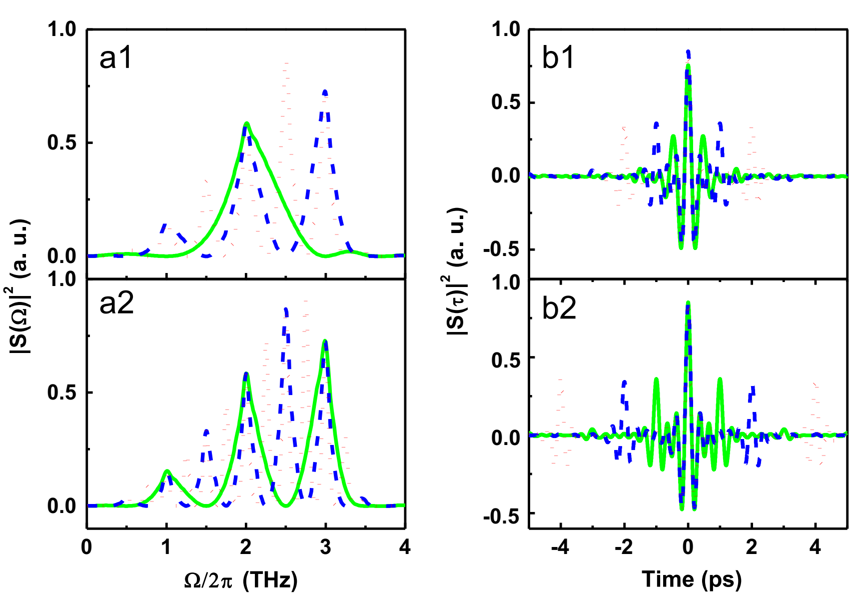

Fig. 5. The terahertz spectra $|S(\Omega)|^2$ induced by the shaped femtosecond laser pulses with the modulation depths $\alpha=0.5\pi$ (a-1) and π (a-2) for the modulation periods $\beta=0.5$ THz (red dotted line), 1 (blue dashed line) and 2 (green solid line), and the corresponding terahertz waveforms $|S(\tau)|^2$ (b-1) and (b-2). (For interpretation of the references to color in this figure legend, the reader is referred to the web version of this article.)

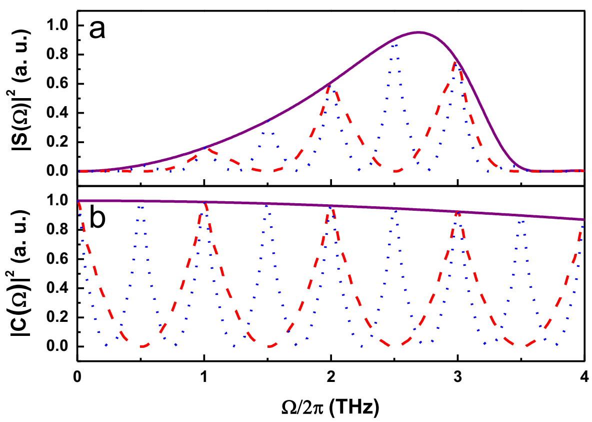

Fig. 6. The terahertz spectra $|S(\Omega)|^2$ (a) and the power spectra $|C(\Omega)|^2$ (b) induced by the transform-limited femtosecond laser pulses (purple solid line) and the shaped femtosecond laser pulses with the modulation period $\beta = 1$ THz for the modulation depths $\alpha = 0.5\pi$ (red dashed line) and π (blue dotted line). (For interpretation of the references to color in this figure legend, the reader is referred to the web version of this article.)

$\tau_{mod} = 1/\beta$ at $\alpha = 0.5\pi$ and $\tau_{mod} = 2/\beta$ at $\alpha = \pi$, these relations is very helpful for pre-designed terahertz pulses.

Finally, in order to explore the physical control mechanism of the shaped and tunable terahertz pulse generation in Figs. 3–5, we compare the terahertz spectrum $|S(\Omega)|^2$ with the power spectrum $|C(\Omega)|^2$ since the terahertz pulse shape depends on the power spectrum of the shaped femtosecond laser pulses (see Eqs. (3) and (4)). Fig. 6 presents the terahertz spectra $|S(\Omega)|^2$ (a) and the power spectra $|C(\Omega)|^2$ (b) induced by the transform-limited femtosecond laser pulses (purple solid line) and the shaped femtosecond laser pulses with the modulation period $\beta = 1$ THz for the modulation depths $\alpha = 0.5\pi$ (red dashed line) and π (blue dotted line). One can see from Fig. 6(b) that the power spectrum $|C(\Omega)|^2$ is periodically modulated and the modulation period is also 1 THz at $\alpha = 0.5\pi$ and 0.5 THz at $\alpha = \pi$, which is the same as the terahertz spectrum (see Fig. 6(a)). Obviously, the power spectrum $|C(\Omega)|^2$ can well explain the terahertz spectral modulation. Similarly, the terahertz waveform modulation can also be explained by considering the Fourier transform of the power spectrum $|C(\Omega)|^2$.

In conclusion, we have theoretically shown that, by the square spectral phase modulation, the terahertz pulse generation via optical rectification in ZnTe crystal can be effectively controlled. It was shown that the terahertz spectrum is periodically modulated and the terahertz pulses are split into multiple subpulses, and the modulation period of the terahertz spectrum and the relative intensity and time interval of the terahertz subpulses can be continuously tuned. It was also shown that the physical control mechanism of the shaped and tunable terahertz pulse generation can be well explained by considering the power spectrum of the shaped femtosecond laser pulses. We believe that these theoretical results can serve as a basis for further experimental study, and are also expected to be significant for the related applications in various fields.

This work was partly supported by National Natural Science Fund (No. 11004060, No. 11027403 and No. 51132004) and Shanghai Rising-Star Program (No. 12QA1400900).

References

[1] D.H. Auston, P.R. Smith, Applied Physics Letters 43 (1983) 631.
[2] Ch. Fattinger, D. Grischkowsky, Applied Physics Letters 54 (1989) 490.
[3] D.H. Auston, K.P. Cheung, J.A. Valdmanis, D.A. Kleinman, Physical Review Letters 53 (1984) 1555.
[4] M.D. Thomson, M. Kreß, T. Löffler, H.G. Roskos, Laser and Photonics Reviews 1 (2007) 349.
[5] N. Karpowicz, X. Lu, X.-C. Zhang, Journal of Modern Optics 56 (2009) 1137.
[6] P.Y. Han, G.C. Cho, X.-C. Zhang, Optics Letters 25 (2000) 242.
[7] J.L. Johnson, T.D. Dorney, D.M. Mittleman, Applied Physics Letters 78 (2001) 835.
[8] T. Kleine-Ostmann, T. Nagatsuma, Journal of Infrared, Millimeter and Terahertz Waves 32 (2) (2011) 143.
[9] H.-J. Song, T. Nagatsuma, IEEE Transactions on Terahertz Science and Technology 1 (2011) 256.
[10] E. Knoesel, M. Bonn, J. Shan, T.F. Heinz, Physical Review Letters 86 (2001) 340.
[11] C. Rønne, P. Astrand, S.R. Keiding, Physical Review Letters 82 (1999) 2888.
[12] D.S. Citrin, Applied Physics Letters 76 (2000) 3176.
[13] M.Y. Su, S.G. Carter, M.S. Sherwin, A. Huntington, L.A. Coldren, Applied Physics Letters 81 (2002) 1564.
[14] D.D. Arnone, C.M. Ciesla, A. Corchia, S. Egusa, M. Pepper, J.M. Chamberlain, C. Bezant, E.H. Linfield, Proceedings of SPIE 3828 (1999) 209.
[15] Z.D. Taylor, R.S. Singh, D.B. Bennett, P. Tewari, C.P. Kealey, N. Bajwa, M.O. Culjat, A Stojadinovic, H. Lee, J.-P. Hubschman, E.R. Browm, W.S. Grundfest, IEEE Transactions on Terahertz Science and Technology 1 (1) (2011) 201.
[16] J.B. Jackson, M. Mourou, J.F. Whitaker, I.N. Duling III, S.L. Williamson, M. Menu, G.A. Mourou, Optics Communications 281 (2008) 527.
[17] T. Qi, Y.-H. Shin, K.-L. Yeh, K.A. Nelson, A.M. Rappe, Physical Review Letters 102 (2009) 247603.
[18] Y.-S. Lee, T.B. Norris, Journal of the Optical Society of America B 19 (2002) 2791.
[19] Y.-S. Lee, N. Amer, W.C. Hurlbut, Applied Physics Letters 82 (2003) 170.
[20] J.Y. Sohn, Y.H. Ahn, D.J. Park, E. Oh, D.S. Kim, Applied Physics Letters 81 (2002) 13.
[21] J. Ahn, A.V. Efimov, R.D. Averitt, A.J. Taylor, Optics Express 11 (2003) 2486.
[22] S. Vidal, J. Degert, J Oberlé, E. Freysz, Journal of the Optical Society of America B 27 (2010) 1044.
[23] S. Zhang, M. Wu, C. Lu, T. Jia, Z. Sun, Physical Review A 84 (2011) 043419.
[24] B. Dayan, A. Pe'er, A.A. Friesem, Y. Silberberg, Physical Review Letters 93 (2004) 023005.
[25] S. Zhang, Z. Wang, Z. Sun, Chinese Physics B 17 (2008) 2914.
[26] J.-P. Caumes, L. Videau, C. Rouyer, E. Freysz, Physical Review Letters 89 (2002) 047401.
[27] G. Gallot, D. Grischkowsky, Journal of the Optical Society of America B 16 (1999) 1204.